ATTITUDE CONTROL OF A NANO QUADROTOR

Luis Otávio Guedes Lobo e Silva*, Antonio Eduardo Carrilho da Cunha*

**Programa de Pós Graduação em Engenharia Elétrica (PGEE)*
Instituto Militar de Engenharia (IME)
Praça Gen. Tibúrcio, 80, Praia Vermelha
22290-270, Rio de Janeiro, RJ, Brazil

Emails: luis.cefet.rj@gmail.com, carrilho@ime.eb.br

Abstract— This paper presents a proposal for attitude control of a quadrotor using a cascade control architecture. The control objective is to maintain the quadrotor at a fixed position in three-dimensional space using the available onboard sensors. The control strategy consists of using an inner loop to stabilize the orientation and the height of the quadrotor and an outer loop to stabilize the horizontal position using the linear speeds as reference signals.

Keywords— Attitude Control, Quadrotor.

Resumo— Este artigo apresenta uma proposta para o controle de atitude de um quadricóptero usando uma arquitetura de controle do tipo cascata. O objetivo é manter o quadricóptero no ar em uma posição fixa no espaço tridimensional, usando os sensores embarcados disponíveis. A estratégia de controle consiste em utilizar uma malha interna para estabilizar a orientação e a altura do quadricóptero e uma malha externa para estabilizar a posição horizontal, utilizando as velocidades lineares como sinais de referência.

Palavras-chave— Controle de Atitude, Quadricóptero.

1 Introduction

The widespread and increasing use of drones in many different applications is now a reality. We are concerned with the high number of accidents already reported with both civilian and military drones. For instance, from 2003 to 2013 US military drones were involved in around 400 accidents during operations (Whitlock, 2014). Among the causes, the premature deployment of not enough tested devices and the suppression of some security subsystems or sensors in order to get quickly a new product with less cost are noteworthy in the engineer perspective. We consider thus that the investigation of drone technology and control techniques is a relevant task.

One of the most fundamental control task when considering a drone system is the attitude control. It is an essential control loop that regulates angular orientations and linear speeds of the device in order to make it more *stable* to perform high level control tasks. For instance, by making first the drone being stable in a fixed 3D space position it is possible to, in a higher level control loop, make it move from one point to the other or to follow a specified trajectory. The attitude control is fundamental for both remote piloting and autonomous flight. It relies mostly onboard sensors like an inertial measurement unit (IMU), equipped accelerometers, rate gyros and magnetometers, or additional onboard sensors like barometers or sonars.

We work with quadrotors for some reasons. First, currently there are many affordable drone systems based on quadrotors. Second, because the control actuation is relatively simple, based on the speeds of the rotors. Nevertheless, the task to control them is still a challenge. Quadrotors are underactuated nonlinear systems with coupling of control modes and many difficulties in modelling, like the aerodynamics of propellers. Third, when compared with other drone systems, the quadrotor can perform interesting maneuvers like vertical take off and landing (VTOL) or hovering. Moreover, they are suitable for indoors or outdoors environments. We work with the Crazyflie platform from Bitcraze [1], a light (19g) and very small (9 cm from rotor to rotor) open source platform.

We can find a lot of works that deal with attitude control of quadrotors such as (Mueller and D'Andrea, 2014; Tayebi and McGilvray, 2006; Raffo et al., 2009; Basri et al., 2014; Martin and Salaüm, 2010; Bouabdallah, 2007; Hanna, 2014; Costa, 2012; Borges et al., 2015; Lebedev, 2013). Our model is based on the modelling presented in (Beard, 2008; Lebedev, 2013). However, we have obtained a relatively satisfactory control result by ignoring the air resistance and the rotor drag proposed on (Hanna, 2014; Leishman et al., 2014; Martin and Salaüm, 2010), the uncertainties in (Basri et al., 2014) and the quaternions in (Tayebi and McGilvray, 2006; Borges et al., 2015).

In this work we propose an attitude controller that tries to exploit the maximum possible from the quadrotor onboard sensors by maintaining the quadrotor at a stable 3D position in space. The control objective is to maintain the quadrotor at a fixed position in three-dimensional space using the available onboard sensors. For instance, the

[1]https://www.bitcraze.io/crazyflie/

Crazyflie has an accelerometer, a rate gyro, a magnetometer and a barometer. Using the onboard sensor fusion routines (Martin and Salaün, 2010) we can obtain relatively accurate estimates of the quadrotor angular orientation and height. We propose a two layered attitude control where we use additional information on the linear speeds. It can be shown that without the feedback of the linear speeds, it is not possible to attain to a fixed 3D position (Lobo e Silva, 2016).

This paper is organized as follows: In section 2 we report the modelling of the quadrotor. In section 3 we describe the linearization of the system. In section 4 we explain the synthesis of the inner and outer loops controls. In section 5 we show the simulation results of the outer loop control. In section 6 we present a tracking test of the controllers implemented on the Crazyflie and in section 7 we show our conclusion.

2 Mathematical Modelling of the Crazyflie

Figure 1 shows a schematic model of a quadrotor frame in the cross "+" configuration . There are four motors R_i, $i = 1...4$. The front rotor R_1 and the back rotor R_3 spin clockwise, the right rotor R_2 and the left rotor R_4 spin counter-clockwise. Figure 1 also shows the main coordinates frames in this work, the body frame (x_b, y_b, z_b) attached to the body of the device and the inertial frame (x_i, y_i, z_i) attached to a fixed ground reference.

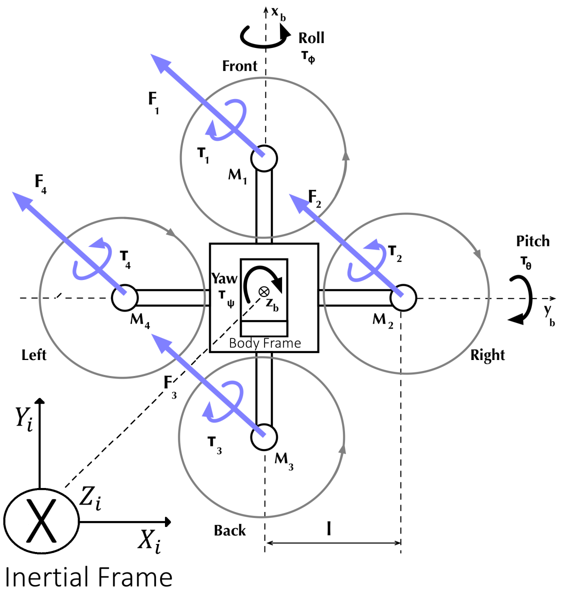

Figure 1: Crazyflie top view.

The motors generate at the frame a thrust F_i and a torque τ_i according to the direction of rotation. We suppose that the thrust F_i and toque τ_i are related to the PWM duty cycle of the actuators δ_i, with $\delta_i \in [0, 1]$, by $F_i = k_f \delta_i$ and $\tau_i = k_f \delta_i$, where k_f and k_t are the thrust and torque constants.

For control purposes, we define the total thrust (F) and the roll (τ_ϕ), pitch(τ_θ) and yaw (τ_ψ) torques as:

$$\begin{aligned} F &= F_1 + F_2 + F_3 + F_4 \\ \tau_\phi &= l(F_4 - F_2) \\ \tau_\theta &= l(F_1 - F_3) \\ \tau_\psi &= \tau_1 + \tau_3 - \tau_2 - \tau_4 \end{aligned} \tag{1}$$

where l is the distance from the rotors to the center of mass.

The following set of nonlinear equations that describes the quadrotor dynamics can be obtained by application of Newton-Euler or Lagrangian methods as can be followed in (Beard, 2008).

$$\begin{aligned} \dot{p}_n &= u(cos(\theta)cos(\psi)) + v(sin(\phi)sin(\theta)cos(\psi) \\ &- cos(\phi)sin(\psi)) - w(sin(\phi)sin(\psi) \\ &+ cos(\phi)cos(\psi)sin(\theta)) \\ \dot{p}_e &= u(cos(\theta)sin(\psi)) + v(sin(\phi)sin(\theta)sin(\psi) \\ &+ cos(\phi)cos(\psi)) - w(cos(\phi)sin(\psi)sin(\theta) \\ &- cos(\psi)sin(\phi) \\ \dot{h} &= -wcos(\phi)cos(\theta) - usin(\theta) + vcos(\theta)sin(\phi) \\ \dot{u} &= rv - qw - gsin(\theta) \\ \dot{v} &= pw - ru + gcos(\theta)sin(\phi) \\ \dot{w} &= qu - pv - F/m + gcos(\phi)cos(\theta) \\ \dot{\phi} &= p + rcos(\phi)tan(\theta) + qsin(\phi)tan(\theta) \\ \dot{\theta} &= qcos(\phi) - rsin(\phi) \\ \dot{\psi} &= rcos(\phi)/cos(\theta) + qsin(\phi)/cos(\theta) \\ \dot{p} &= \tau_\phi/J_x + qr(J_y - J_z)/J_x \\ \dot{q} &= \tau_\theta/J_y + pr(J_x - J_z)/J_y \\ \dot{r} &= \tau_\psi/J_z + pq(J_x - J_y)/J_z \end{aligned} \tag{2}$$

The state variables are the following: The *Inertial Positions* $\vec{P} = [p_n \ p_e \ h]^T$ measured in meters with respect to the inertial frame, where p_n is the north position, p_e is the east position and h is the height position. The *Linear speeds* $\vec{V} = [u \ v \ w]^T$ measured in meters per second with respect to the body frame, where u is the longitudinal speed, v is the lateral speed and w is the vertical speed. The *angular orientations* $\vec{\omega} = [\phi \ \theta \ \psi]^T$ represented by the *Euler angles*, measured in radians with respect to a sequence of rotations in order to obtain the body frame from the inertial frame (Beard, 2008), where ϕ is the roll angle, θ is the pitch angle and ψ is the yaw angle. The *angular rates* $\vec{\Omega} = [p \ q \ r]^T$ measured in radians per second with respect to the body frame, where p is the roll rate, q is the pitch rate and r is the yaw rate.

The parameters for the Crazyflie 1.0 are: The mass of quadrotor (m = 1.875×10^{-2} [Kg]), the acceleration of gravity (g = 9.81 [m/s^2]), the distance from the rotor to the center of mass (l = 4.25×10^{-2} [m]), the thurst constant of rotor ($k_f = 8.62 \times 10^{-2}$ [N/units]), the torque constant of rotor ($k_t = 4.2823 \times 10^{-4}$ [N.m/units]) and the moments of inertia with respect to x_b ($J_x = 1.81 \times 10^{-5}$), y_b ($J_y = 1.82 \times 10^{-5}$) and z_b ($J_z = 1.92 \times 10^{-5}$ [$Kg.m^2$]). The constants k_f and k_t were obtained from experiments in (Borges et al., 2015). The other parameters were either directly measured or estimated.

3 Linearization

For control purpose, we define a state vector $\vec{X} = [p_n\ p_e\ h\ u\ v\ w\ \phi\ \theta\ \psi\ p\ q\ r]^T$ and an input vector $\vec{U} = [F'\ \tau'_\phi\ \tau'_\theta\ \tau'_\psi]^T$.

The nonlinear equations can be linearized around an equilibrium point $(\vec{X}_0, \vec{U}_0)$ for small signals, with the state $\vec{x}$ and the input $\vec{u}$ for the system $\vec{X} = \vec{X}_0 + \vec{x}$ and $\vec{U} = \vec{U}_0 + \vec{u}$, where $\vec{x}$ and $\vec{u}$ are the linearized state and input respectively.

Let's start the definition of an equilibrium point corresponding to the quadrotor at a static position in the 3D space by arbitrating:

$$\begin{aligned} u_0 = v_0 = w_0 = &\ 0 \quad [m/s] \\ p_0 = q_0 = r_0 = &\ 0 \quad [rad/s] \end{aligned} \tag{3}$$

By applying the above conditions to the nonlinear system equations $\dot{\vec{X}} = f(\vec{X}, \vec{U})$, the following values turn the remaining derivatives null:

$$\begin{aligned} F'_0 = &\ mg/k_f \quad [N] \\ \tau'_{\phi_0} = \tau'_{\theta_0} = \tau'_{\psi_0} = &\ 0 \quad [N.m] \\ \phi_0 = \theta_0 = &\ 0 \quad [rad] \end{aligned} \tag{4}$$

Note that the derivatives are null independently from the value of p_n, p_e, h and ψ. The equilibrium point is then:

$$\begin{aligned} \vec{X}_0 &= [p_{n_0}\ p_{e_0}\ h_0\ 0\ 0\ 0\ 0\ 0\ \psi_0\ 0\ 0\ 0]^T \\ \vec{U}_0 &= [mg/k_f\ 0\ 0\ 0]^T \end{aligned} \tag{5}$$

where $(p_{n_0}, p_{e_0}, h_0) \in \mathbb{R}^3$, in meters, and $\psi_0 \in \mathbb{R}$. We have arbitrated $\psi_0 = 0$ rad.

We follow a procedure indicated in (Borges et al., 2015) by defining lumped parameters:

$$\begin{aligned} \sigma_\phi \triangleq lk_f/J_x \quad \sigma_\psi \triangleq k_t/J_z \\ \sigma_\theta \triangleq lk_f/J_y \quad \sigma_h \triangleq k_f/m \end{aligned} \tag{6}$$

and generalized forces:

$$\begin{aligned} F' \triangleq F/k_f \quad \tau'_\theta \triangleq \tau_\theta/lk_f \\ \tau'_\phi \triangleq \tau_\phi/lk_f \quad \tau'_\psi \triangleq \tau_\psi/k_t \end{aligned} \tag{7}$$

As doing this we will concentrate all the model parametric uncertainty into single lumped parameters, allowing us to analyse the robustness of our controller design in future steps. Second, the generalized forces are now defined in units compatible to the dimension of the PWM duty cycle.

With these equations we have that:

$$\begin{aligned} F' = \delta_1 + \delta_2 + \delta_3 + \delta_4 \quad \tau'_\theta = \delta_1 - \delta_3 \\ \tau'_\psi = \delta_1 + \delta_3 - \delta_2 - \delta_4 \quad \tau'_\phi = \delta_4 - \delta_2 \end{aligned} \tag{8}$$

Applying a linearization method around the equilibrium point, as indicated in (Franklin et al., 2013), the linear state equations are:

$$\begin{aligned} \dot{p_n} = u \quad & \dot{u} = -g\theta \quad & \dot{\phi} = p \quad & \dot{p} = \sigma_\phi \tau'_\phi \\ \dot{p_e} = v \quad & \dot{v} = g\phi \quad & \dot{\theta} = q \quad & \dot{q} = \sigma_\theta \tau'_\theta \\ \dot{h} = -w \quad & \dot{w} = -\sigma_h F' \quad & \dot{\psi} = r \quad & \dot{r} = \sigma_\psi \tau'_\phi \end{aligned} \tag{9}$$

The linearized model is composed of simple first order differential equations. The decoupling of the variables in (9) is exploited in the control design. Observe there are four main decoupled modes, as shown figure 2.

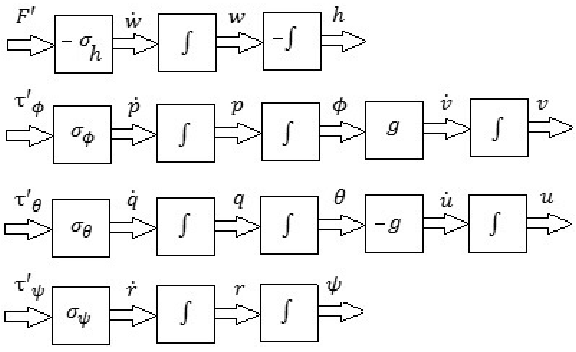

Figure 2: Linear model block diagram.

We call these modes as follows. The height mode connects the thrust F'_0 to the vertical speed w and the height h. The yaw mode connects the yaw torque τ'_ψ to the yaw rate r and yaw angle ψ. The lateral mode connects the roll torque τ'_ϕ to the roll rate p, roll angle ϕ and lateral speed v. The longitudinal mode connects the pitch torque τ'_θ to the pitch rate q, pitch angle θ and longitudinal speed u. We will exploit this decomposition in the controller design.

4 Controller Design

4.1 Overview

We work with a cascade control architecture. An inner loop is responsible for stabilization by regulation the Euler angles ϕ, θ, ψ and the vertical height h. It can be shown that this controller solely is unable to stabilize the quadrotor at a horizontal position. Considering the possibility of estimating the linear speeds u and v from accelerometer data, as indicated in (Leishman et al., 2014), we propose an external control loop to regulate the horizontal speeds u and v. The outer loop uses u and v as reference to determine the set point for the inner loop. Besides, it is possible to use different control strategies for the outer loop unaffecting the inner loop. The proposal architecture is then shown in figure 3.

4.2 Inner Loop

We consider the following controllers for the inner control loop: the Pitch control regulates the pitch angle θ; the Roll control regulates the roll angle ϕ; The Yaw control regulates the yaw angle ψ. These three controllers use data from the sensor fusion algorithm. Finally, Height control uses the vertical speed to stabilize the height.

ISSN 2525-8311

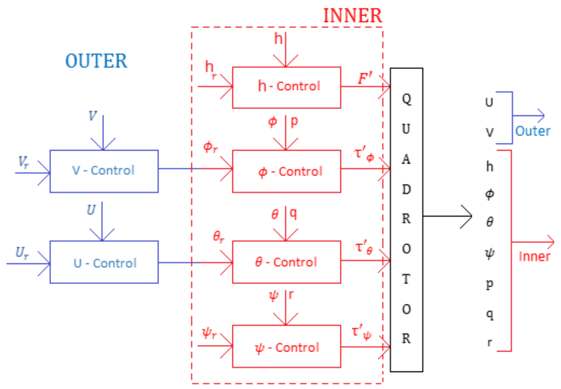

Figure 3: Decoupling mode.

In this paper we describe only the pitch mode synthesis. The roll, yaw and height modes are analogous to the pitch mode.

According with equation (9), the pitch mode corresponds to the following state-space representation:

$$\begin{bmatrix} \dot{\theta} \\ \dot{q} \end{bmatrix} = \begin{bmatrix} 0 & 1 \\ 0 & 0 \end{bmatrix} \begin{bmatrix} \theta \\ q \end{bmatrix} + \begin{bmatrix} 0 \\ \sigma_\theta \end{bmatrix} \tau'_\theta \qquad (10)$$

The structure of the pitch controller is defined in figure 4 that corresponds to a full state feedback with robust tracking by integral error (Franklin et al., 2013). This control scheme leads to zero steady state error for steps reference input. The reference θ_r is given to the desired pitch angle θ.

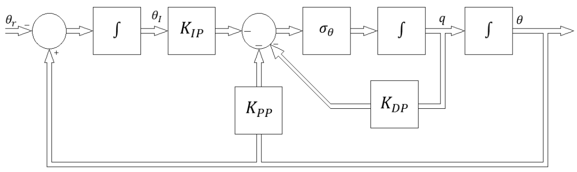

Figure 4: Block diagram for pitch control.

In the control scheme of figure 4, the integral state is defined by:

$$\dot{\theta}_I = \theta - \theta_r \qquad (11)$$

Then, the resulting control law is:

$$\tau'_\theta = -K_{IP}\theta_I - K_{PP}\theta - K_{DP}q \qquad (12)$$

Observe that the control law consists implicity of a proportional action K_{PP}, an integral action K_{IP} and a derivative action K_{DP}.

The inner loop controllers were sinthesized using the LQR techniques (Franklin et al., 2013). The LQR weighting matrices were adjusted by checking the steps response of the system. One of the main constrains was to maintain the control action τ'_θ in order to maintain the PWM duty cycles δ_i in the range [0,1]. From equation 8, we can estimate that the generalized pitch torque τ'_θ can be decoded into the rotors PWM duty cycle $\delta_1 = F'_0 + \tau'_\theta$ and $\delta_3 = F'_0 - \tau'_\theta$, where we use $F'_0 \triangleq mg/k_f$ as the standard value to maintain the quadrotor in the air. From this, we can see that the control action of the other controller loop act as disturbances. In order to make the integral control, all the system were augmented of one integral state as indicated in (Franklin et al., 2013). The controllers gains and closed loop poles are shown in table 1.

Table 1: Table of poles and gains for inner loop.

Mode	*poles*	K_I	K_P	K_D
Roll	$-0.86638 \pm 0.50061i$ -20.216	0.1	0.17801	0.10844
Pitch	$-0.86638 \pm 0.50062i$ -20.0104	0.1	0.17804	0.10848
Yaw	$-0.88626 \pm 0.56825i$ -2.0123	0.1	0.20962	0.16970
H	-0.83460 ± 0.66885 -1.2709	0.31623	0.71026	-0.63952

4.3 Outer Loop

For the outer control loop we consider the following modes: The U controller inspired in the dependence of u and θ in equation (9), and the V controller inspired in the dependence of v and ϕ in equation (9).

The structure of the U controller is defined in figure 5. As well as pitch controller, the U control has a full state feedback with robust tracking by integral error. The reference u_r is given to the desired longitudinal speed u. The main idea is to use the output of the U controlles θ_r as a reference to the pitch controller. The V mode is analogous to the U mode.

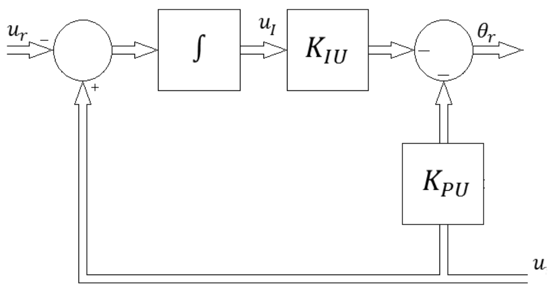

Figure 5: Block diagram for U control.

The U and V controllers were also sinthesied by LQR. The weighting matrices were adjusted by trial and error, by observing system step response. The restriction were to make the U and V dynamics slower than the inner loop and the restriction on the value as the outputs θ_r and ϕ_r based on the typical values of the inner loop controller. The results are in table 2.

Table 2: Table of poles and gains for outer loop.

Mode	*poles*	K_I	K_P
U	-0.10647 -0.29138	$-3.1623 \cdot 10^{-3}$	$-4.0555 \cdot 10^{-2}$
V	-0.10647 -0.29138	$3.1623 \cdot 10^{-3}$	$4.0555 \cdot 10^{-2}$

5 Simulations

We perform a simulation of the controllers in closed loop against the nonlinear model.

As an initial condition to the simulation we define the following: $p_n = p_e = h = 0$ [m], $u = v = w = 0$ [m/s], $\phi = 0.1$ [rad], $\theta = -0.3$ [rad], $\psi = 0.2$ [rad] and $p = q = r = 0$ [rad/s]. The reference inputs are: $u_r = v_r = h_r = 0$ [m/s] and $\psi_r = 0$ [rad]. The simulation time is 40s.

The simulation responses of the outer loop system are shown in figures 6, 7 and 8.

We conclude that the quadrotor hovers in a fixed position. After 20 seconds, the positions p_n and p_e remain in a fix value. All the Euler angles and all the angular rates have the same settling time in 5 seconds. Also, due to integral action, the steady state errors for the linear speeds, the euler angle and the angular rates are all null. Finally, the values of δ_1, δ_2, δ_3 and δ_4 are between 0 and 1. It can be shown that, without the U and V controllers, the horizontal position cannot be stabilized (Lobo e Silva, 2016).

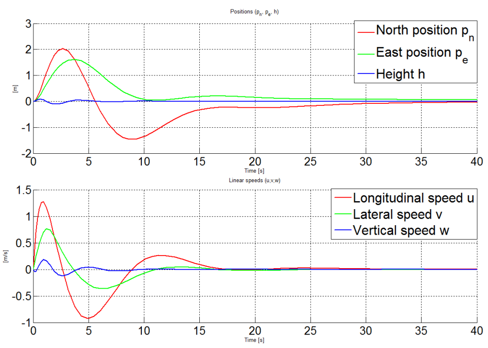

Figure 6: Positions and linear speeds.

6 Implementation and Tests

We have implemented the roll, pitch and yaw controllers on the real quadrotor. First, we tied the quadrotor between two support columns in a way to allow only the pitch movement, as in figure 9.

The main idea is to check if the output θ tracks the reference input θ_r. Finally, we have compared the results of the simulation with the real recorded data. The results are shown in figure 10. We have obtained similar result for the roll and yaw controllers.

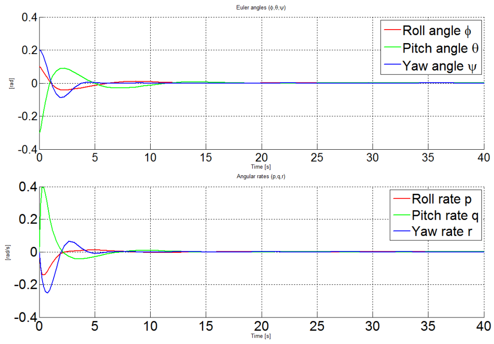

Figure 7: Euler angles and angular rates.

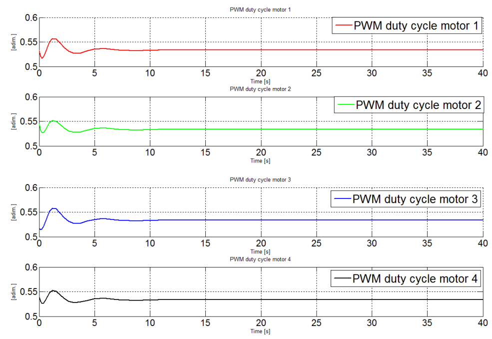

Figure 8: PWM Duty Cycles

Despite of the wind force generated by the rotation of the propellers causes oscillations at the quadrotor, observe that the recorded θ tracks the reference signals.

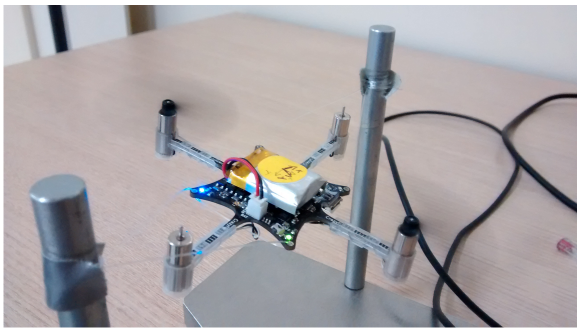

Figure 9: Crazyfle tied between to columns for pitch control test.

The figure 11 shows a flying performance data for the attitude control. The results show that the h state tracks the reference h_r and the speeds u and v oscillate around the reference signal with maximum values of $|u_{max}| = 0.4$ $[m/s]$ and $|v_{max}| = 0.7$ $[m/s]$. Although the outer loop replaces θ_r and ϕ_r for u_r and v_r respectively, the Euler angles states oscillate close to zero [rad]. Due to the arguments presented, the outer loop provides a good regulation of the position.

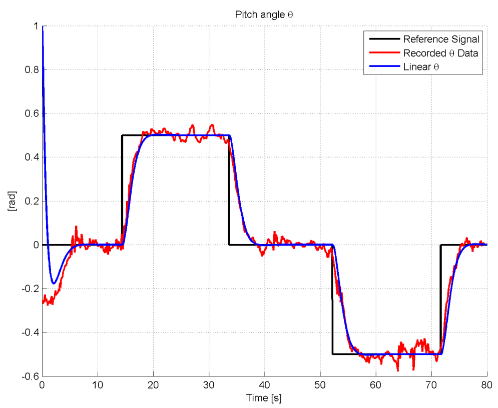

Figure 10: Comparison between measured data and simulation (pitch mode).

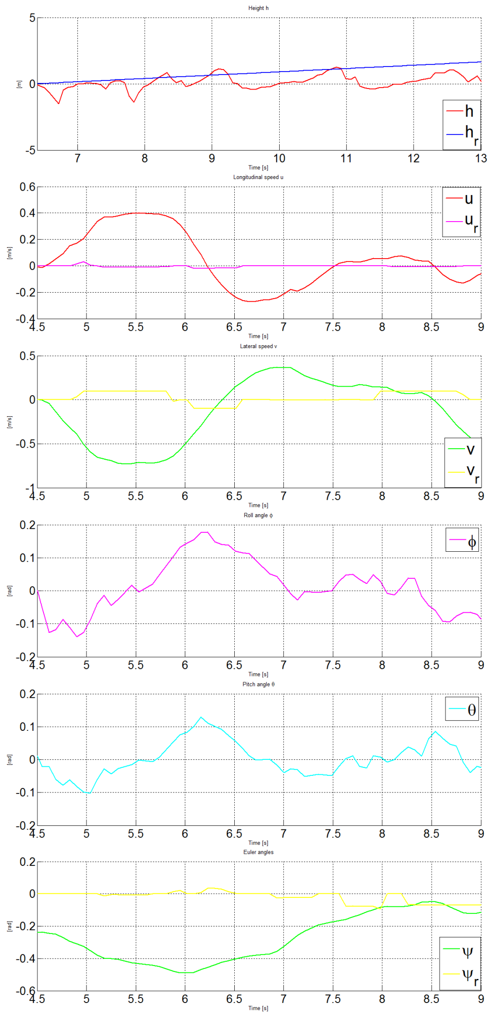

Figure 11: Real flight data.

7 Conclusion

This paper presents an attitude control using decoupling modes to perform each movement of the quadrotor independently. A LQR controller with integral action was designed for each mode to optimizing the dynamics responses. Also, utilizing the longitudinal and lateral speeds as reference signals allow the quadrotor hovers in a fixed height in 3D space without using external position sensors.

In future work, the authors intend to implement a Kalman Filter for estimating the longitudinal and lateral speeds to improve the performance of the controller.

Acknowledgements

We expose our acknowledgements to: the technician *Victor Luiz Dias de Castro* for support and maintenance of Crazyflies and *Coordenação de Aperfeiçoamento de Pessoal de Nível Superior* (CAPES) for financial support of research.

References

Basri, M. A. M., Husain, A. R. and Danapalasingam, K. A. (2014). *Intelligent Adaptive Backstepping Control for MIMO Uncertain Nonlinear Quadrotor Helicopter System*, pp. 311 – 314. DOI: 10.1177/0142331214538900.

Beard, R. W. (2008). *Quadrotor Dynamics and Control*, Brigham Young University. Available at http://hdl.lib.byu.edu/1877/624b.

Borges, L. M., de Moura Magalhães, G. and dos Santos, E. G. (2015). *Controle de Atitude de um Quadricoptero*, Instituto Militar de Engenharia.

Bouabdallah, S. (2007). *Design and Control of Quadrotors with Application to Autonomous Flying*, Master's thesis, École Polytechnique Fédérale de Lausanne.

Costa, E. B. (2012). *Algoritmos de Controle Aplicados á Estabilização do Voo de um Quadrotor*, Master's thesis, Universidade Federal de Juiz de Fora.

Franklin, G. F., Powell, J. D. and Emami-Naenini, A. (2013). *Sistemas de Controle para Engenharia*, Bookman.

Hanna, W. (2014). *Modelling and Control of an Unmanned Aerial Vehicle*, Master's thesis, Charles Darwin University.

Lebedev, A. (2013). *Design and Implementation of a 6DOF Control System for an Autonomous Quadrocopter*, Master's thesis, Universität Würzburg.

Leishman, R. C., Jr., J. C. M., Beard, R. W. and Mclain, T. W. (2014). *Quadrotors and Accelerometers - State Estimation with and Improved Dynamic Model*, **34**: 28 – 41. DOI: 10.1109/MCS.2013.2287362.

Lobo e Silva, L. O. G. (2016). *Attitude control of a nano quadcopter*, Master's thesis, Instituto Militar de Engenharia.

Martin, P. and Salaüm, E. (2010). *The True Role of Acceleration Feedback in Quadrotor Control* . Available at https://hal.archives-ouvertes.fr/hal-00422423v2.

Mueller, M. W. and D'Andrea, R. (2014). *Stability and control of a quadrocopter despite the complete loss of one, two or three propellers.* DOI: 10.1109/ICRA.2014.6906588.

Raffo, G. V., Ortega, M. G. and Rubio, F. R. (2009). *An integral predictive/nonlinear H_∞ control structure for a quadrotor helicopter*, *Automatica* **46**: 29 – 39. DOI: 10.1016/j.automatica.2009.10.018.

Tayebi, A. and McGilvray, S. (2006). *Attitude Stabilization of a VTOL Quadrotor Aircraft*, *IEEE Transactions on Control Systems Magazine* **14**(3): 562 – 571. DOI: 10.1109/TCST.2006.872519.

Whitlock, C. (2014). *When Drones Fall from the Sky*, *Washington Post* . Available at http://www.washingtonpost.com/sf/investigative/2014/06/20/when-drones-fall-from-the-sky/.